

Supporting Information

A Ratiometric Fluorescent Probe for *in situ* Quantification of Basal Mitochondrial Hypochlorite in Cancer Cells

Ji-Ting Hou, Kun Li,* Jin Yang, Kang-Kang Yu, Ye-Xin Liao, Yu-Zhao Ran, Yan-Hong Liu,
Xue-Dong Zhou* and Xiao-Qi Yu*

E-mail addresses: kli@scu.edu.cn; xqyu@scu.edu.cn

Content

Experimental section	S2
Synthesis of RMClO-1 and RMClO-2	S3-4
Figure S1 Absorption spectra of RMClO-1 and RMClO-2 toward ROS	S5
Figure S2 Fluorescence spectra of RMClO-1 and RMClO-2 toward ROS under single excitation	S5
Figure S3 Fluorescence spectra of RMClO-1 and RMClO-2 toward ROS under dual excitation	S6
Figure S4 Fluorescence spectra of RMClO-1 and RMClO-2 toward cations	S6
Figure S5 Effect of pH on the reaction of RMClO-1 or RMClO-2 with ClO ⁻	S7
Figure S6 Temporal profile of fluorescence of RMClO-1 or RMClO-2 with ClO ⁻	S7
Figure S7 ESI spectra of RMClO-1 upon addition of ClO ⁻	S8
Figure S8 Confocal imaging of HeLa cells with RMClO-1 or RMClO-2 .	S8
Figure S9 Confocal imaging of RMClO-1 in other cells	S9
Figure S10 Effects of RMClO-2 on the viability of A549 cells	S9
Figure S11 Confocal imaging of ClO ⁻ in HeLa cells with RMClO-2	S10
Figure S12 Fluorescence images of ClO ⁻ -blocking cancer cells with RMClO-2	S10
Figure S13 Confocal fluorescence images of endogenous ClO ⁻ in RAW 264.7 cells	S11
NMR and MS copies of various compounds	S12 -16

Experimental Section

General remarks for experimental

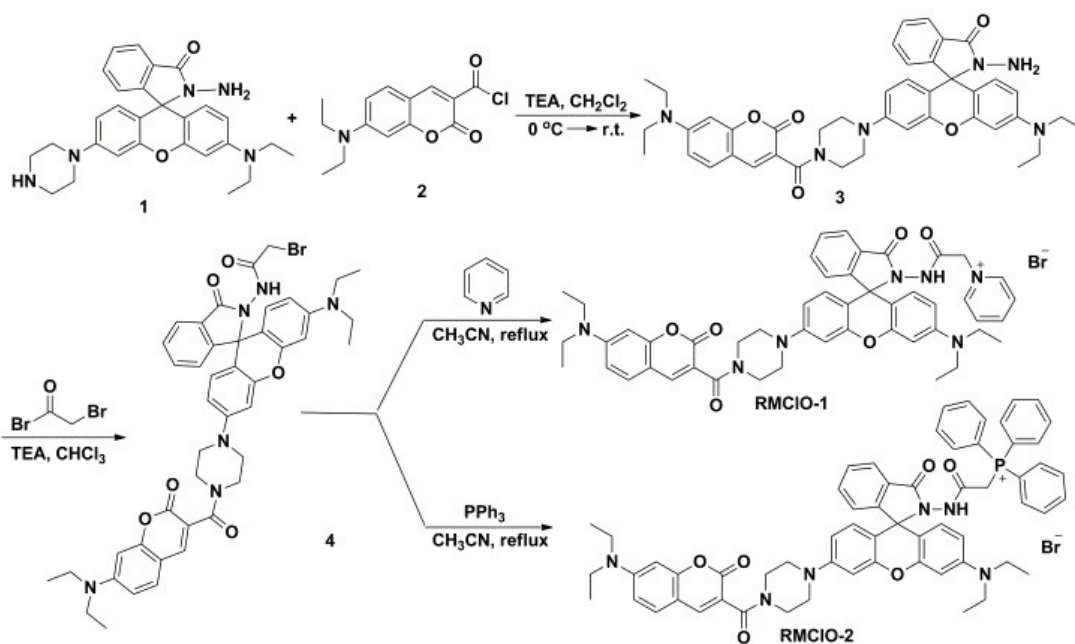
^1H NMR, ^{13}C NMR spectra were measured on a Bruker AM400 NMR spectrometer. Proton Chemical shifts of NMR spectra were given in ppm relative to internal reference TMS (^1H , 0.00 ppm). ESI-MS and HRMS spectral data were recorded on a Finnigan LCQ^{DECA} and a Bruker Daltonics Bio TOF mass spectrometer, respectively. All pH measurements were performed with a pH-3c digital pH-meter (Shanghai Lei Ci Device Works, Shanghai, China) with a combined glass-calomel electrode. Fluorescence emission spectra were obtained using FluoroMax-4 Spectrofluorophotometer (HORIBA Jobin Yvon) at 298 K. Unless otherwise noted, materials were obtained from commercial suppliers and were used without further purification. All the solvents were dried according to the standard methods prior to use. All of the solvents were either HPLC or spectroscopic grade in the optical spectroscopic studies.

Determination of ROS. The concentration of H_2O_2 was determined from the absorption at 240 nm ($\epsilon = 43.6 \text{ M}^{-1}\text{cm}^{-1}$) in PBS. The concentration of ONOO^- was determined from the absorption at 302 nm ($\epsilon = 1670 \text{ M}^{-1}\text{cm}^{-1}$) in 0.1 N NaOH. The concentration of ClO^- was determined from the absorption at 292 nm ($\epsilon = 350 \text{ M}^{-1}\text{cm}^{-1}$) in PBS. $\bullet\text{OH}$ was generated at 25 °C by means of the Fenton reaction with H_2O_2 and a 10-fold excess of $\text{Fe}(\text{ClO}_4)_2$.

Fluorescence analysis. Probes **RMClO-1** and **RMClO-2** were prepared in DMSO at a concentration of 5 mM. All UV/Vis and fluorescence titration experiments were performed using 5 μM **RMClO-1** or **RMClO-2** in PBS buffer solution (pH 7.4, 10 mM) with varying concentrations of analytes at room temperature. Fluorescence emission spectra were obtained with a Xenon lamp and 1.0 cm quartz cells.

Confocal imaging of living cells. All cells were cultured in Dulbecco's modified Eagle medium (DMEM) containing 10% fetal bovine serum and 1% Antibiotic-Antimycotic at 37 °C in a 5% CO_2 /95% air incubator. For fluorescence imaging, cells (4×10^3 /well) were passed on a 6-well plate and incubated for 24h. After the treatment of cells, the imaging was carried out on Leica TCS SP8.

Synthesis of RMCIO-1 and RMCIO-2.



Compound **1** and **2** were synthesized according to the literature.^{1,2}

Preparation and Characterization of **3**

A solution of compound **2** (279 mg, 1.0 mmol) in 5 mL of dry CH₂Cl₂ was added batch-wise to a solution of compound **1** (469 mg, 1.0 mmol) and triethylamine (TEA) (111 mg, 1.1 mmol) in 20 mL of dry CH₂Cl₂ stirred in an ice bath. After the addition, the reaction mixture was warmed to the room temperature and stirred overnight. The solvent was removed under reduced pressure and the crude product was purified by column chromatography over silica gel eluting with CH₂Cl₂/CH₃CO₂C₂H₅ = 5:1 to afford yellow solid. Yield: 544 mg, 76.4%. ¹H NMR (400 MHz, DMSO-*d*₆) δ 8.02 (s, 1H), 7.82 – 7.74 (m, 1H), 7.55 – 7.44 (m, 3H), 7.02 – 6.95 (m, 1H), 6.79 – 6.71 (m, 2H), 6.66 (dd, *J* = 8.8, 2.4 Hz, 1H), 6.58 (d, *J* = 2.2 Hz, 1H), 6.43 (d, *J* = 8.8 Hz, 1H), 6.40–6.29 (m, 3H), 4.34 (s, 2H), 3.72 (s, 2H), 3.49 – 3.44 (m, 6H), 3.34 – 3.20 (m, 8H), 1.14 (t, *J* = 7.0 Hz, 6H), 1.09 (t, *J* = 7.0 Hz, 6H). ESI-MS: *m/z* 713.5 [M + H]⁺.

Preparation and Characterization of **4**

A solution of 2-bromoacetyl bromide (145 mg, 0.72 mmol) in 5 mL of dry CH₂Cl₂ was added drop-wise to a solution of compound **3** (342 mg, 0.48 mmol) and TEA (97 mg, 0.96 mmol) in 20 mL of dry CH₂Cl₂ stirred in an ice bath. After the addition, the reaction mixture was warmed to the room temperature and stirred overnight. The solvent was removed under reduced pressure and the crude product was purified by column chromatography over silica gel eluting with CH₂Cl₂/CH₃CO₂C₂H₅ = 8:1 to afford yellow solid. Yield: 320 mg, 80%. ¹H NMR (400 MHz, DMSO-*d*₆) δ 9.99 (s, 1H), 8.02 (s, 1H), 7.85 (dd, *J* = 6.4, 1.8 Hz, 1H), 7.64 – 7.46 (m, 3H), 7.04 (d, *J* = 8 Hz, 1H), 6.76 (dd, *J* = 9.0, 2.2 Hz, 1H), 6.70 – 6.62 (m, 2H), 6.62 – 6.55 (m, 2H), 6.49 (d, *J* = 8.0 Hz, 1H), 6.42 – 6.30 (m, 2H), 3.76 (s, 2H), 3.71 (s, 2H), 3.50 – 3.44 (m, 6H), 3.36 – 3.21 (m, 8H), 1.14 (t, *J* = 7.0 Hz, 6H), 1.08 (t, *J* = 7.0 Hz, 6H). ¹³C NMR (100 MHz, DMSO-*d*₆) δ 165.26, 164.54, 163.79, 158.91, 157.11, 153.36, 153.15, 151.86, 151.74, 144.43, 133.95, 130.61, 129.23, 128.88, 124.37, 123.23, 116.26, 109.88, 107.60, 101.94, 96.78, 65.33, 60.22, 44.65, 28.51, 27.25.

21.23, 14.56, 12.77. HRMS calcd for $C_{44}H_{45}BrN_6O_6$ $[M + H]^+$: 833.2657, found: 833.2654.

Preparation and Characterization of **RMClO-1**

To a solution of **4** (92 mg, 0.11 mmol) dissolved in 10 mL of anhydrous CH_3CN , pyridine (287 μ L, 3.6 mmol) was added in one portion and the reaction solution was heated to reflux for 24 h. Then, the solvent was removed under the reduced pressure and the residue was further purified by column chromatography over silica gel eluting with $CH_2Cl_2/CH_3OH = 20:1$ to afford **RMClO-1** as yellow solid. Yield: 90 mg, 89.6%. 1H NMR (400 MHz, $CDCl_3$) δ 10.46 (s, 1H), 9.00 (d, $J = 5.8$ Hz, 2H), 8.49 (t, $J = 7.8$ Hz, 1H), 7.98 (t, $J = 7.0$ Hz, 2H), 7.88 (s, 1H), 7.82 (d, $J = 7.2$ Hz, 1H), 7.53 – 7.41 (m, 2H), 7.34 (d, $J = 8.8$ Hz, 1H), 7.07 (d, $J = 7.2$ Hz, 1H), 6.69 (d, $J = 8.8$ Hz, 1H), 6.64 – 6.59 (m, 3H), 6.49 (d, $J = 7.2$ Hz, 2H), 6.37 (s, 1H), 6.27 (d, $J = 6.8$ Hz, 1H), 5.74 (s, 2H), 3.83 (s, 2H), 3.53 (s, 2H), 3.44 (q, $J = 8.0$ Hz, 4H), 3.38 – 3.17 (m, 8H), 1.23 (t, $J = 7.2$ Hz, 6H), 1.13 (t, $J = 7.0$ Hz, 6H). ^{13}C NMR (100 MHz, $CDCl_3$) δ 165.06, 164.64, 163.24, 159.29, 157.26, 153.36, 153.21, 151.75, 151.57, 145.88, 145.19, 133.52, 130.03, 129.36, 128.56, 128.11, 127.85, 124.07, 123.44, 115.84, 111.90, 109.45, 108.44, 108.25, 107.75, 102.54, 97.79, 96.91, 66.13, 60.87, 48.67, 48.08, 46.88, 44.97, 44.37, 41.92, 12.67, 12.45. HRMS calcd for $C_{49}H_{50}N_7O_6^+$ $[M]^+$: 832.3817, found: 832.3790.

Preparation and Characterization of **RMClO-2**

To a solution of **4** (92 mg, 0.11 mmol) dissolved in 10 mL of anhydrous CH_3CN , triphenylphosphine (262 mg, 1.0 mmol) was added in one portion and the reaction solution was heated to reflux for 24 h. Then, the solvent was removed under the reduced pressure and the residue was further purified by column chromatography over silica gel eluting with $CH_2Cl_2/CH_3OH = 30:1$ to afford **RMClO-2** as yellow solid. Yield: 110 mg, 91.2%. 1H NMR (400 MHz, $CDCl_3$) δ 10.57 (s, 1H), 7.89 (s, 1H), 7.77 – 7.54 (m, 16H), 7.45 – 7.31 (m, 3H), 6.99 (d, $J = 7.4$ Hz, 1H), 6.79 (d, $J = 8.8$ Hz, 1H), 6.72 (d, $J = 8.9$ Hz, 1H), 6.66 – 6.55 (m, 2H), 6.51 – 6.49 (m, 2H), 6.34 (d, $J = 2.2$ Hz, 1H), 6.29 (d, $J = 8.8$ Hz, 1H), 5.05 (s, 2H), 3.89 (s, 2H), 3.57 (s, 2H), 3.44 (q, $J = 7.0$ Hz, 4H), 3.40 – 3.21 (m, 8H), 1.23 (t, $J = 7.2$ Hz, 6H), 1.16 (t, $J = 7.0$ Hz, 6H). ^{13}C NMR (100 MHz, $CDCl_3$) δ 165.07, 164.65, 161.72, 167.67, 159.27, 157.29, 153.02, 152.89, 152.26, 151.75, 151.62, 148.94, 145.25, 134.87, 133.95, 133.84, 133.23, 130.52, 130.40, 130.12, 129.99, 129.48, 128.14, 127.66, 123.76, 123.36, 118.49, 117.61, 115.91, 112.04, 109.44, 108.78, 108.31, 107.75, 103.68, 102.73, 97.79, 96.91, 65.73, 48.86, 48.27, 44.97, 44.37, 40.92, 31.07, 30.48, 12.69, 12.43. HRMS calcd for $C_{62}H_{60}N_6O_6P^+$ $[M]^+$: 1015.4306, found: 1015.4291.

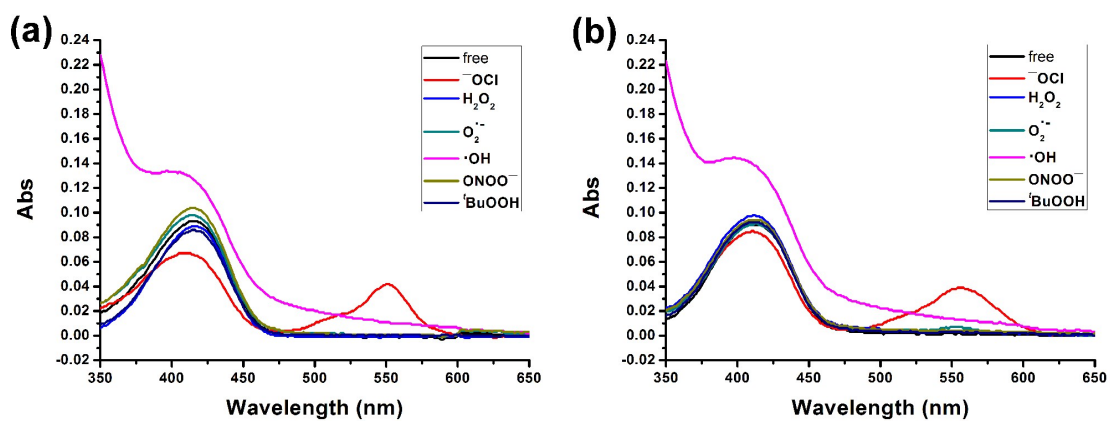


Figure S1. Absorption spectra of (a) **RMCIO-1** and (b) **RMCIO-2** before and after reaction with various ROS in PBS (pH 7.4, 10 mM, containing 0.1% DMSO). $[\text{RMCIO-1}] = [\text{RMCIO-2}] = 5 \mu\text{M}$.

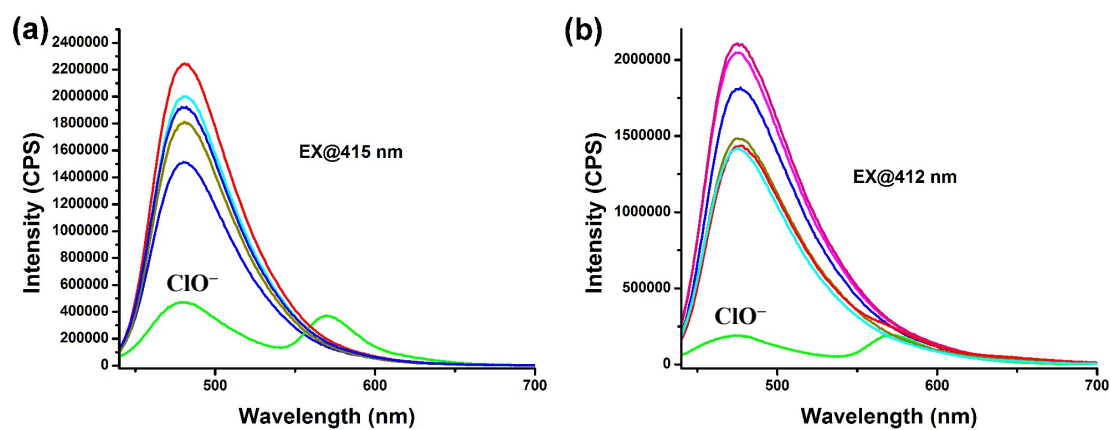


Figure S2. Fluorescence spectra of (a) **RMCIO-1** and (b) **RMCIO-2** before and after reaction with various ROS in PBS (pH 7.4, 10 mM, containing 0.1% DMSO) under single excitation mode. $[\text{RMCIO-1}] = [\text{RMCIO-2}] = 5 \mu\text{M}$; $[\text{ClO}^-] = 100 \mu\text{M}$, $[\text{other ROS}] = 200 \mu\text{M}$.

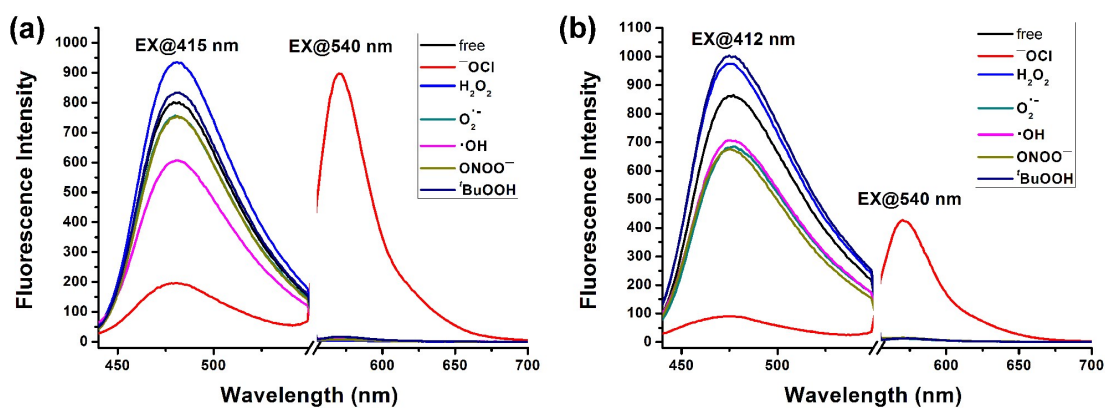


Figure S3. Fluorescence spectra of (a) **RMCIO-1** and (b) **RMCIO-2** before and after reaction with various ROS in PBS (pH 7.4, 10 mM, containing 0.1% DMSO) under dual excitation mode. $[\text{RMCIO-1}] = [\text{RMCIO-2}] = 5 \mu\text{M}$; $[\text{ClO}^-] = 100 \mu\text{M}$, $[\text{other ROS}] = 200 \mu\text{M}$.

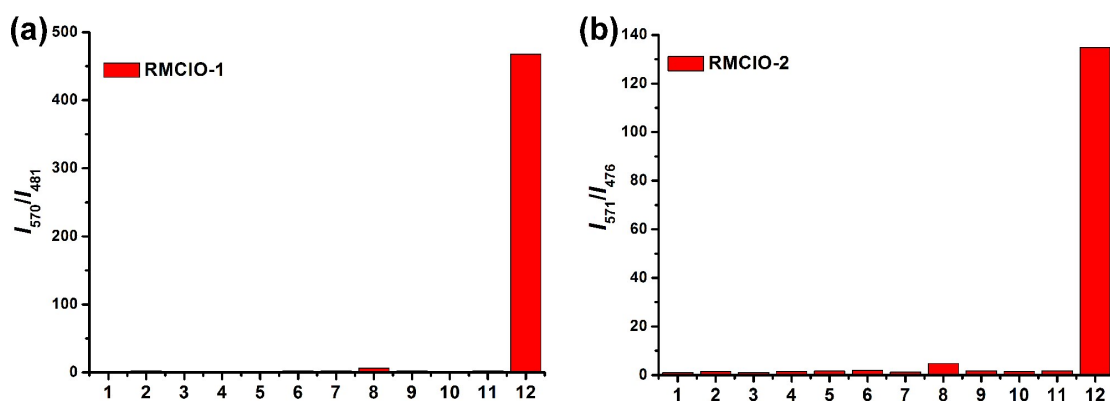


Figure S4. Fluorescence emission intensity ratios of (a) **RMCIO-1** (I_{570}/I_{481}) and (b) **RMCIO-2** (I_{571}/I_{476}) before and after addition of various cations and NaOCl in PBS (pH 7.4, 10 mM, containing 0.1% DMSO). $[\text{Rh-TTP}] = [\text{Rh-Py}] = 5 \mu\text{M}$, $[\text{ClO}^-] = [\text{M}]^{n+} = 100 \mu\text{M}$. 1: blank; 2: Na^+ ; 3: K^+ ; 4: Mg^{2+} ; 5: Fe^{3+} ; 6: Cr^{3+} ; 7: Hg^{2+} ; 8: Pb^{2+} ; 9: Ca^{2+} ; 10: Cu^{2+} ; 11: Zn^{2+} ; 12: ClO^- .

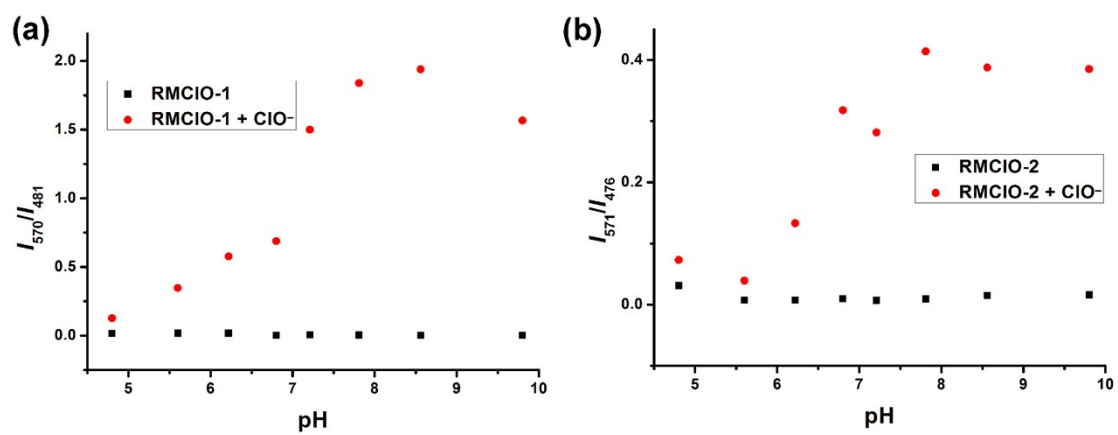


Figure S5. The effect of pH on the emission intensity ratios of (a) **RMCIO-1** (I_{570}/I_{481}) and (b) **RMCIO-2** (I_{570}/I_{476}) in the absence or presence of NaOCl (100 μ M).

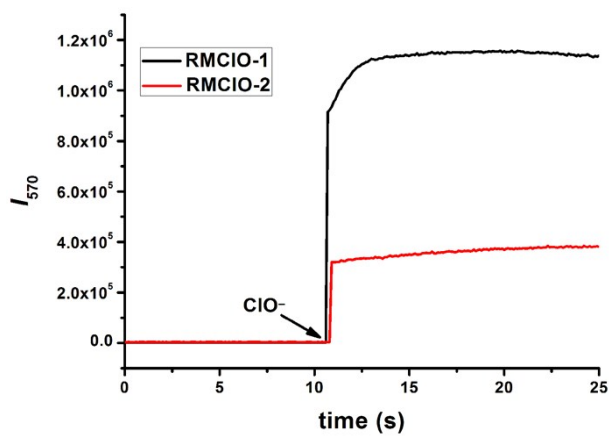


Figure S6. Temporal profile of fluorescence intensity of **RMCIO-1** (black line) and **RMCIO-2** (red line) before and after NaOCl (50 μ M) was added.

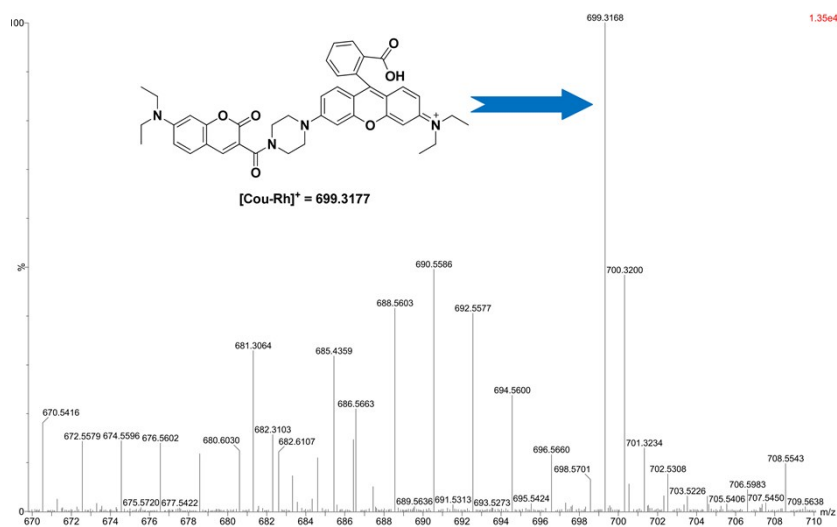


Figure S7. ESI spectra of RMCIO-1 upon addition of 10 equiv ClO⁻.

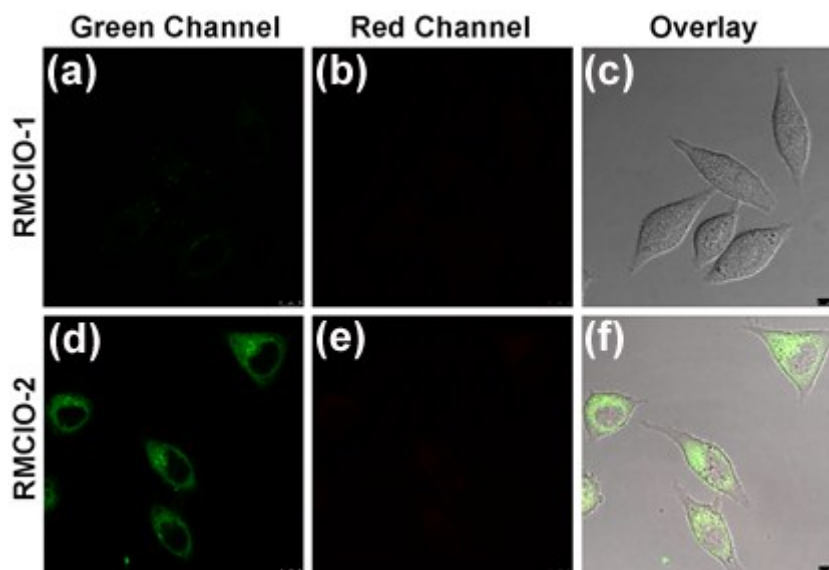


Figure S8. Confocal imaging of HeLa cells with RMCIO-1 or RMCIO-2. HeLa cells were loaded with 5 μ M RMCIO-1 and RMCIO-2 for 30 min. (a) and (d): images of Green Channel excited at 405 nm; (b) and (e): images of Red Channel excited at 552 nm; (c) and (f): merged images. Bars: 10 μ m.

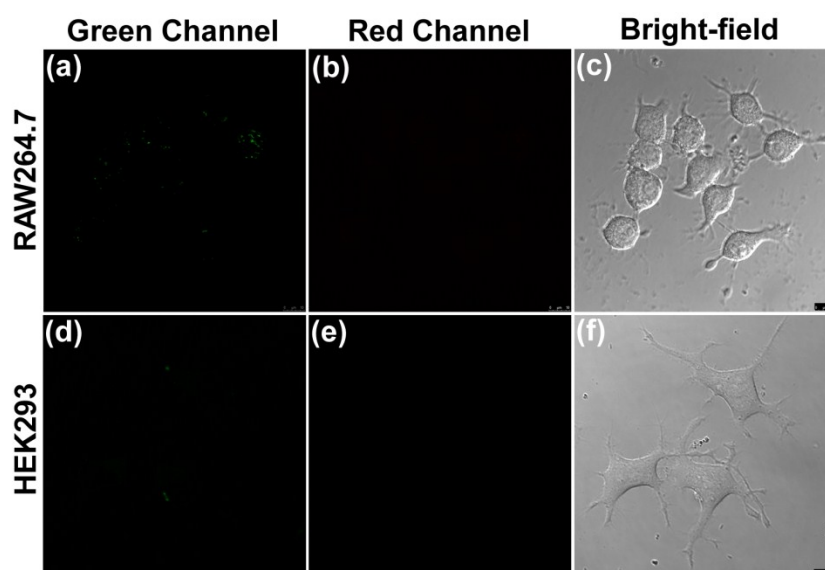


Figure S9. Confocal imaging of **RMCI0-1** in other cells. RAW 264.7 or HEK293 cells were loaded with 5 μM **RMCI0-1** for 30 min, respectively. (a) and (d): images of Green Channel excited at 405 nm; (b) and (e): images of Red Channel excited at 552 nm; (c) and (f): Bright-field images. Bars: 10 μm .

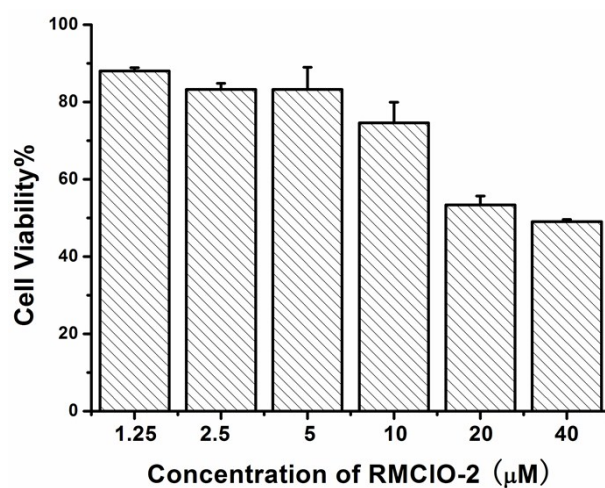


Figure S10. Effects of **RMCI0-2** at varied concentrations on the viability of A549 cells. The results are the mean standard deviation of three separate measurements.

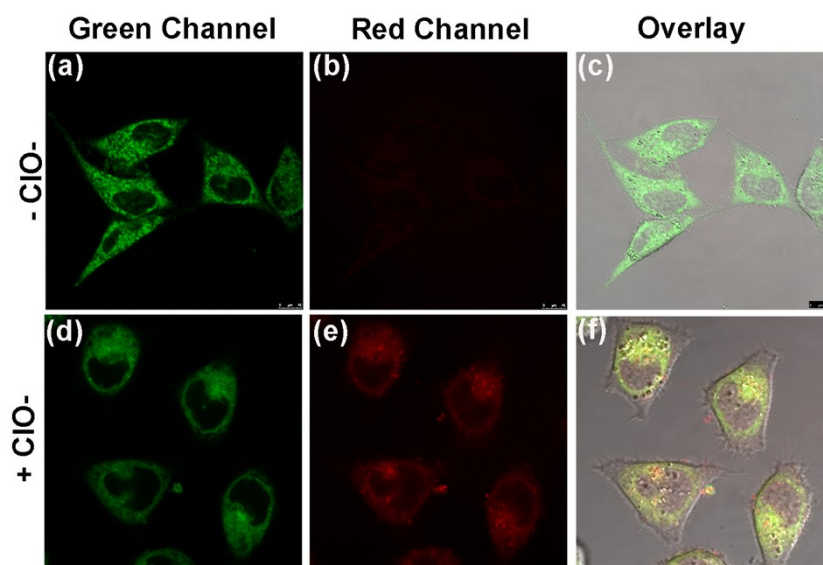


Figure S11. Confocal imaging of ClO⁻ in HeLa cells with **RMCIO-2**. HeLa cells were stained with **RMCIO-2** for 30 min, and then incubated with ClO⁻ (30 μM) for 20 min. (a) and (d): images of Green Channel excited at 405 nm; (b) and (e): images of Red Channel excited at 552 nm; (c) and (f): merged images. Bars: 10 μm.

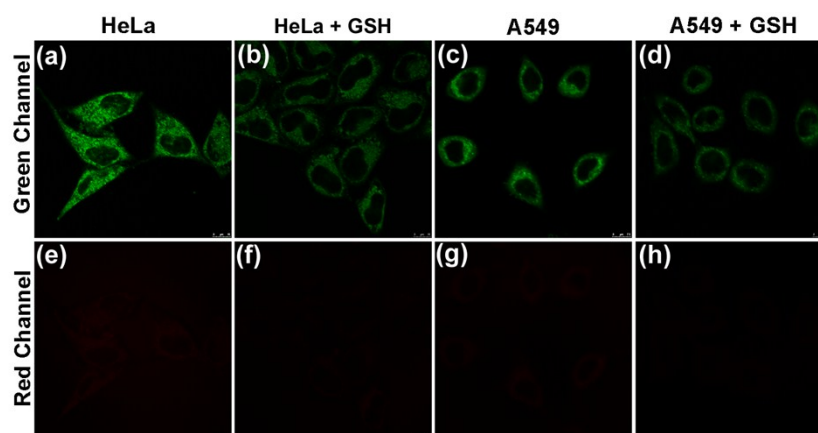


Figure S12. Fluorescence images of ClO⁻-blocking cancer cells after the incubation with 5 μM **RMCIO-2** for 30 min. (a) and (e): HeLa cells; (b) and (f): HeLa +GSH (2 mM, 1 h incubation); (c) and (g): A549 cells; (d) and (h) A549+GSH (2 mM, 1 h incubation). Ex@405 nm for Green Channel from 460 nm to 510 nm; Ex@552 nm for Red Channel from 560 nm to 10 nm. Bars: 10 μm.

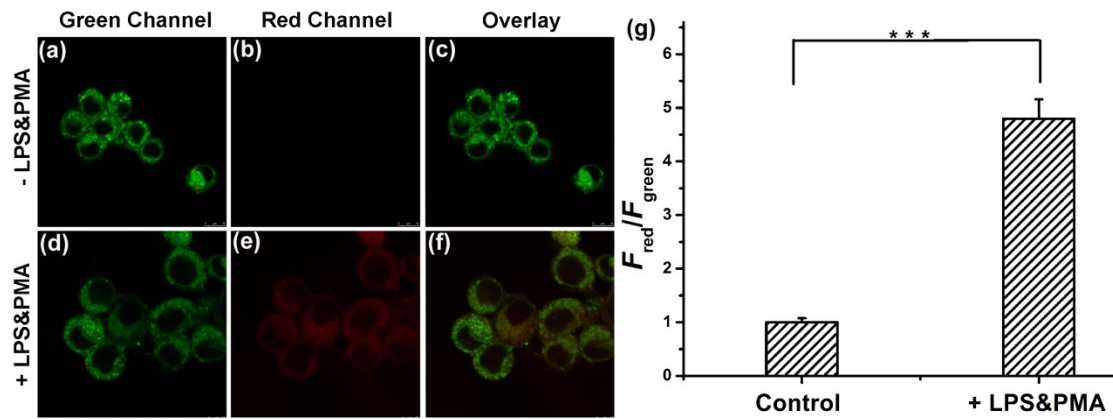
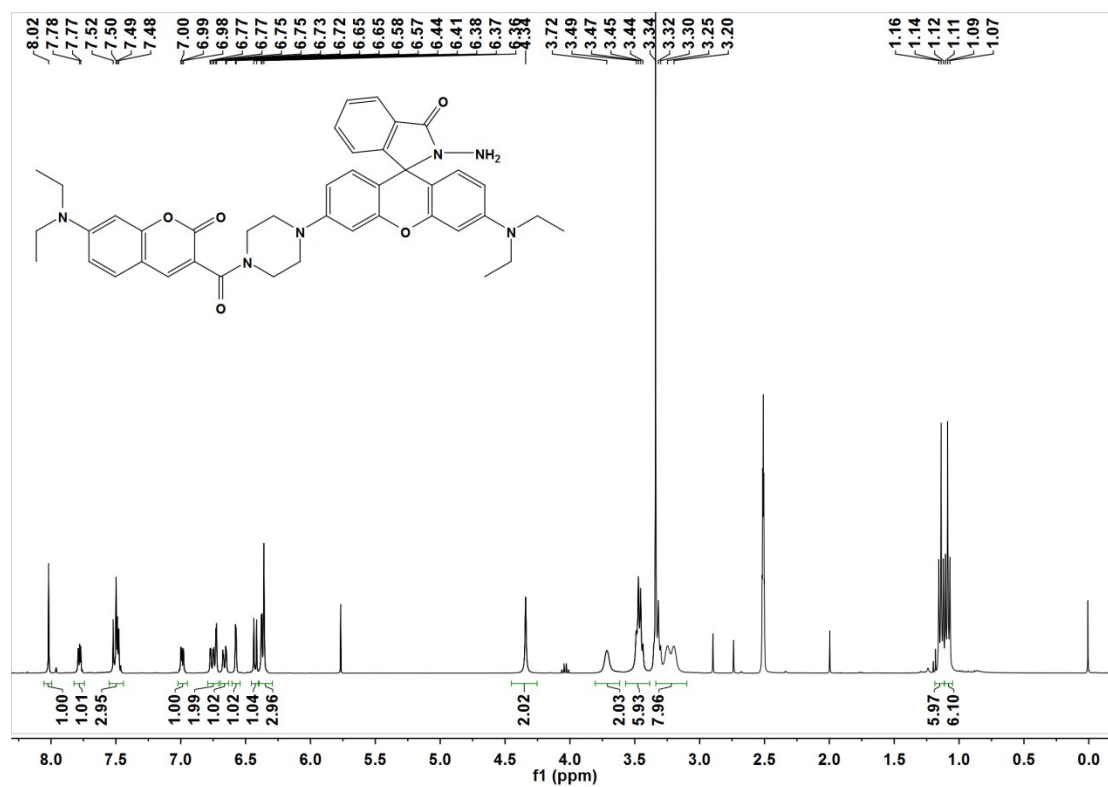
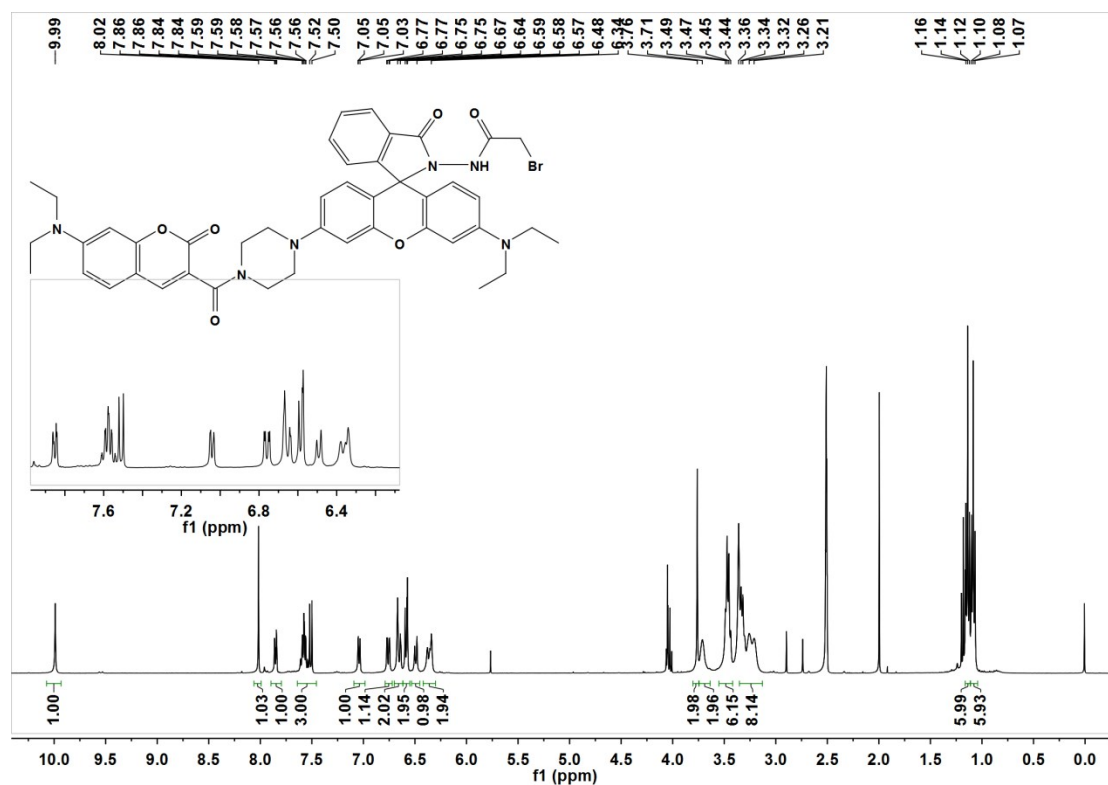


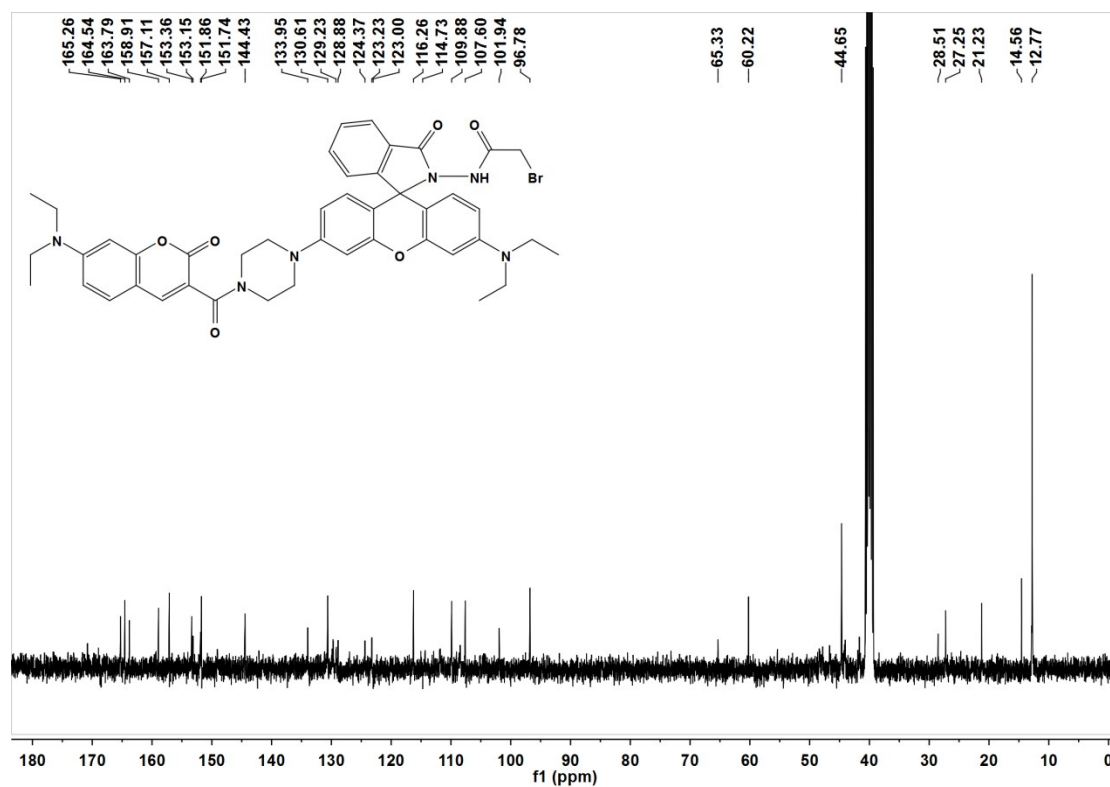
Figure S13 Confocal fluorescence images of RAW 264.7 cells. Cells were stained with LPS (1 $\mu\text{g}/\text{mL}$) for 16 h and were then incubated with PMA (1 $\mu\text{g}/\text{mL}$) for 1 h and were incubated with **RMCI0-2** (5 μM) for 0.5 h. (a) and (d): Green Channel excited at 405 nm (460-510 nm); (b) and (e): Red Channel excited at 552 nm (560-610 nm); (c) and (f): merged images. Bars: 10 μm . (g) Statistical analysis were performed with student's *t*-test ($n = 10$ fields of cells). *** $P < 0.001$.



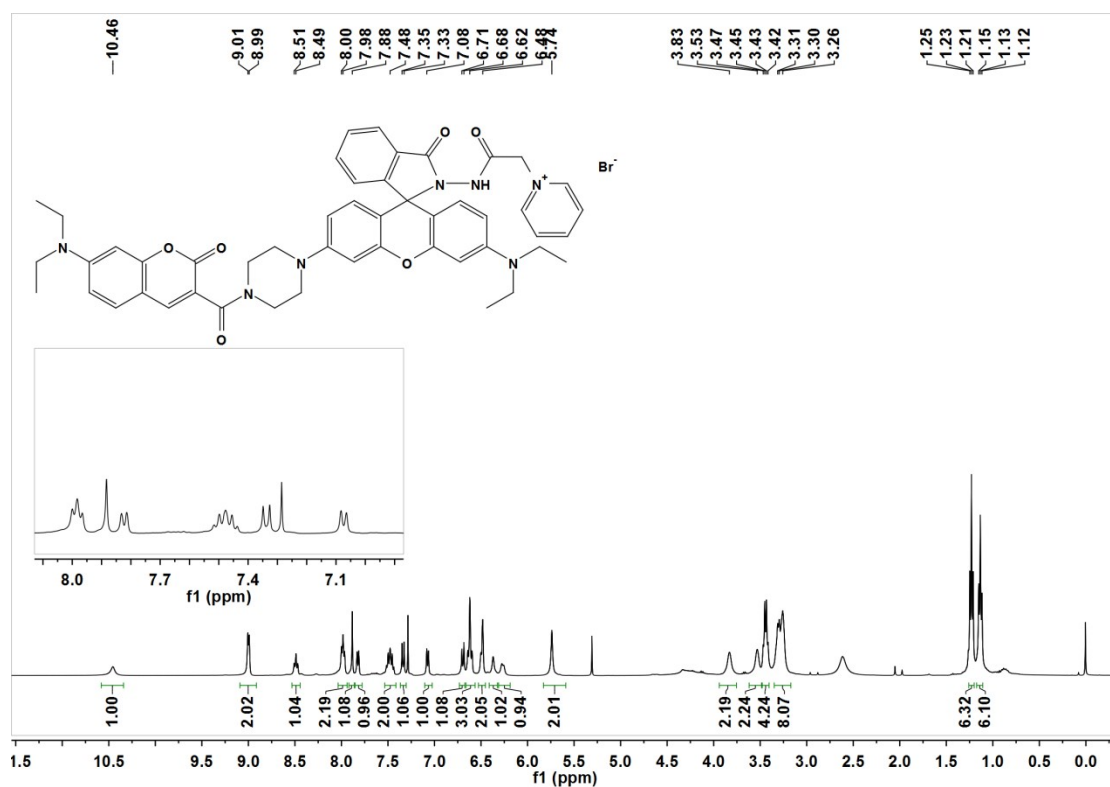
¹H-NMR Spectrum of 3 in DMSO-*d*₆ (400 MHz):



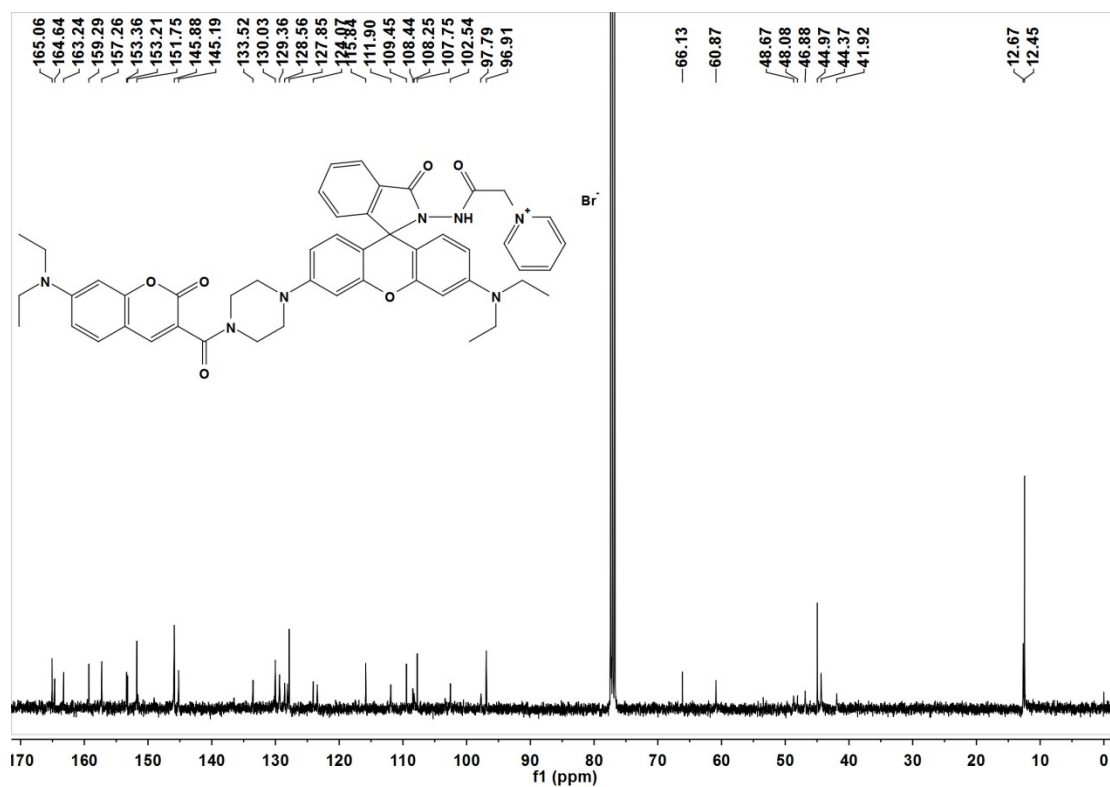
¹H-NMR Spectrum of 4 in DMSO-*d*₆ (400 MHz):



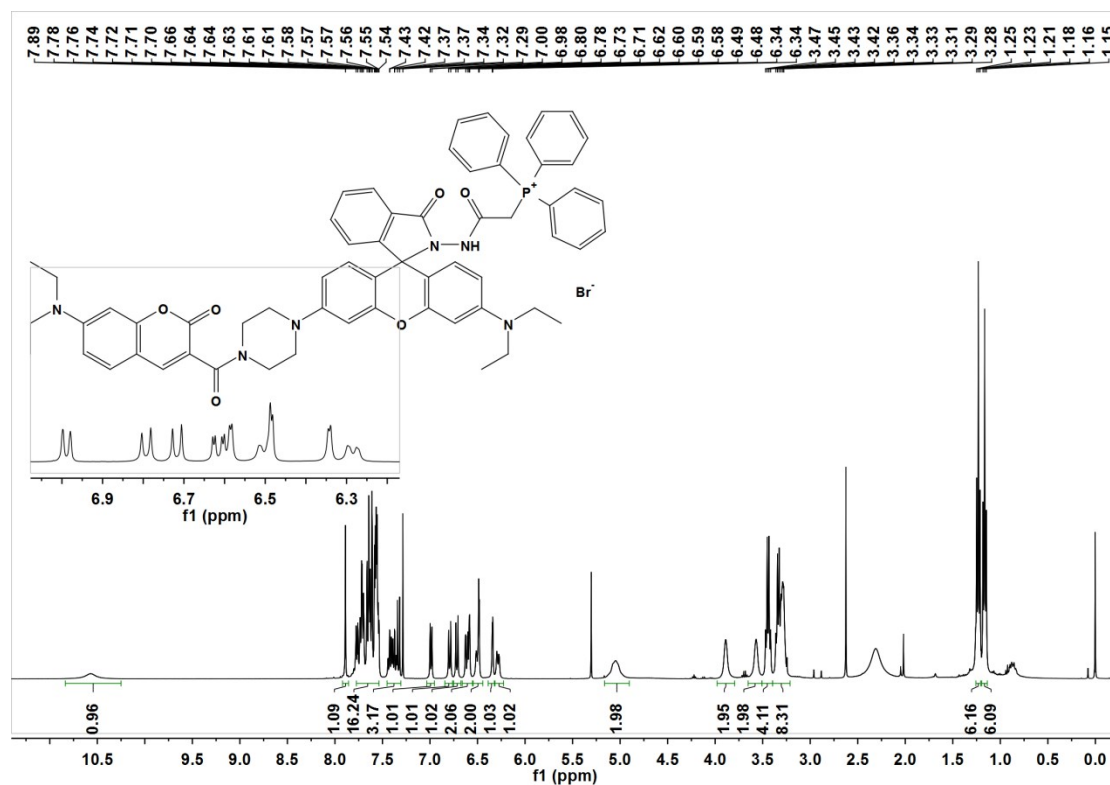
¹³C-NMR Spectrum of 4 in DMSO-*d*₆ (100 MHz):



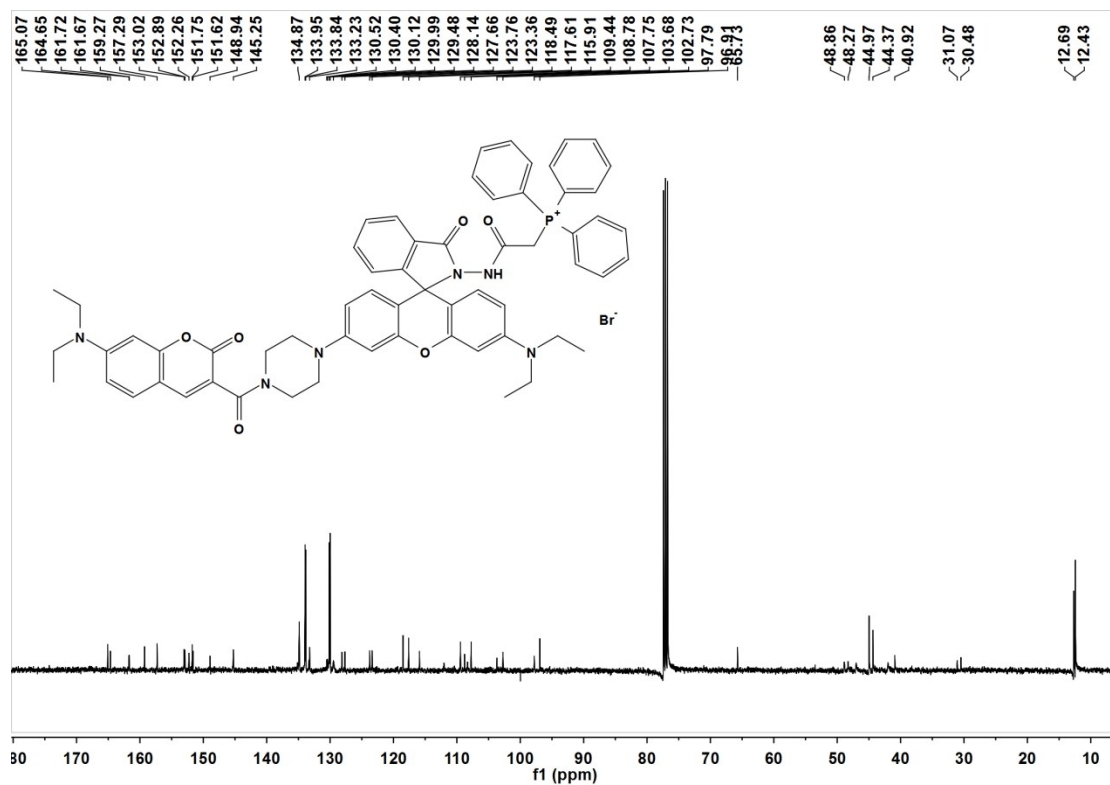
¹H-NMR Spectrum of RMCIO-1 in CDCl₃ (400 MHz):



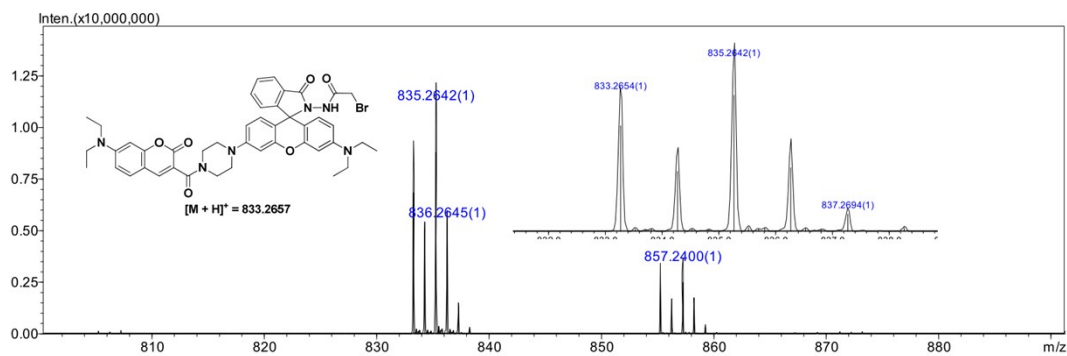
¹³C-NMR Spectrum of **RMCIO-1** in CDCl₃ (100 MHz):



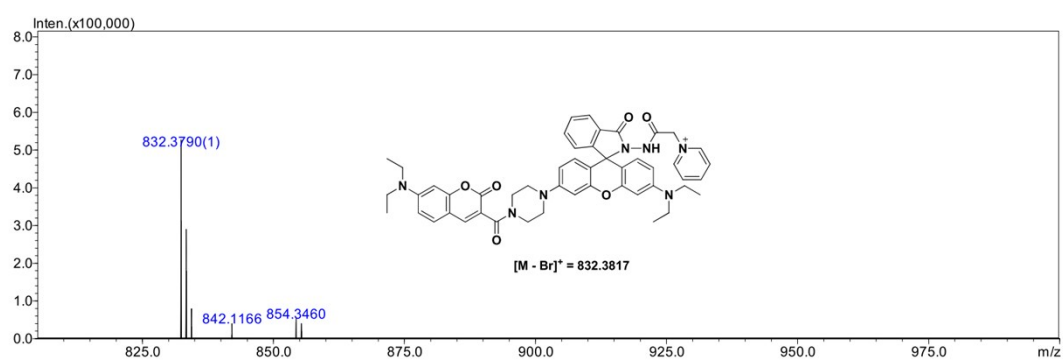
¹H-NMR Spectrum of **RMCIO-2** in CDCl₃ (400 MHz):



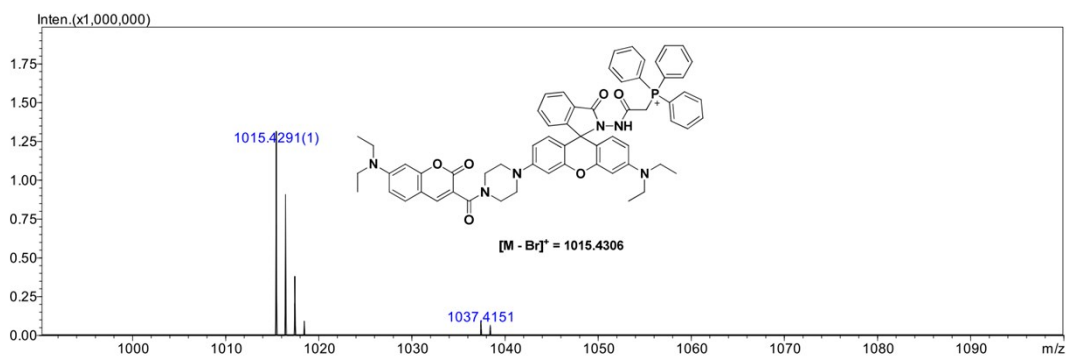
^{13}C -NMR Spectrum of **RMCIO-2** in CDCl_3 (100 MHz):



HRMS spectra of **4**:



HRMS spectra of **RMClO-1**:



HRMS spectra of **RMClO-2**:

Reference

- (1) Zhang, Y.-R.; Chen, X.-P.; Shao, J.; Zhang, J.-Y.; Yuan, Q.; Miao, J.-Y.; Zhao B.-X. *Chem. Commun.* **2014**, *50*, 14241.
- (2) He, G.; Guo, D.; He, C.; Zhang, X.; Zhao, X.; Duan, C. *Angew. Chem. Int. Ed.* **2009**, *48*, 6132.